Reliability Engineering and System Safety 208 (2021) 107440

Contents lists available at ScienceDirect

Reliability Engineering and System Safety

journal homepage: www.elsevier.com/locate/ress

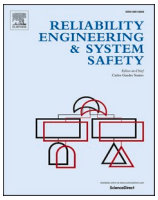

Remaining useful life prediction for degradation with recovery phenomenon based on uncertain process

Sen-Ju Zhang, Rui Kang, Yan-Hui Lin *

School of Reliability and Systems Engineering, Beihang University, Beijing, China

ARTICLE INFO

Keywords:
Uncertainty theory
Recovery phenomenon
Remaining useful life
Epistemic uncertainty
Degradation modeling

ABSTRACT

Remaining useful life prediction based on degradation modeling is of great importance to condition-based maintenance, for which epistemic uncertainty due to the lack of sufficient knowledge needs to be characterized. For certain components, such as the batteries, the recovery phenomenon during degradation has to be considered, and the epistemic uncertainty associated with it is inevitable. This paper proposes a systematic method for degradation modeling and remaining useful life prediction based on uncertain process for degradation with recovery phenomenon. First, uncertain process is adopted for degradation modeling accounting for epistemic uncertainty. Then, a novel similarity based-uncertain weighted least squares estimation method is proposed to update the model parameters with real-time monitoring data. Afterwards, a denoising method is used to deal with the noises caused by recovery phenomenon. Finally, remaining useful life is calculated by uncertain simulation. A case study on real lithium-ion battery degradation dataset is performed to illustrate the effectiveness of the proposed method in comparison with traditional stochastic process.

1. Introduction

Remaining useful life (RUL) is defined as the length of time between the current time and the failure time of an on-site component. The prediction of RUL plays a crucial role in condition-based maintenance (CBM), which is an effective maintenance strategy based on historical information of similar components and on-going information of on-site component [1]. Note that the accuracy of RUL prediction is of great significance in CBM. In practice, components usually demonstrate deteriorating trends before total failure, which is induced by the underlying component degradation process. Therefore, accurate degradation modeling is of great importance.

RUL prediction techniques considering degradation can be mainly divided into two categories: physical model-based method and data-driven method [2]. Physical model-based method involves the adequate knowledge of a device's failure mechanisms and relies heavily on physical principles and engineering experiences [3, 4]. However, detailed physical knowledge of the underlying component degradation processes is hard to be acquired. In contrast, data-driven method does not rely on the precise understanding of nature of degradation. It is commonly used when the degradation data are sufficient and can be mainly divided into two categories: artificial intelligence (AI)-based method and statistical model-based method [5]. AI-based method attempts to learn the degradation patterns from measurements using AI techniques [2]. Usually, AI-based methods are difficult to be explained because they are black-box techniques. Statistical model-based methods set up statistical model based on the historical measurements and update it with accumulated measurements of on-site component, which is easier to be built and explained. Among the developed statistical model-based methods, stochastic process models for characterizing the degradation state have gained much favor due to their ability to characterize stochastic nature of degradation processes [6, 7].

For certain applications, the recovery phenomenon during degradation has to be considered, which has been ignored in most of existing degradation models. One common example refers to the recovery phenomenon in degradation processes of batteries, including lithium-ion batteries and proton exchange membrane fuel cells (PEMFC). For lithium-ion batteries, when batteries rest during charge/discharge profiles, the residual reaction products have a chance to dissipate, thus increasing the available capacity for the next cycle. This phenomenon is called capacity regeneration or self-recovery [8]. For PEMFC, when the stack is stopped for a resting period or characterizations, recoveries can be observed on the power [9].

Uncertainties are characterized as epistemic, if the uncertainties can

* Corresponding author.
E-mail address: linyanhui@buaa.edu.cn (Y.-H. Lin).

https://doi.org/10.1016/j.ress.2021.107440
Received 26 May 2020; Received in revised form 27 November 2020; Accepted 2 January 2021
Available online 6 January 2021

be reduced by gathering more data or by refining models. In this case, as component degradation processes are influenced by many factors, whose exact values may be unknown or partially observed, epistemic uncertainty in uncertain process model method has to be well characterized, which is due to the lack of sufficient knowledge on the degradation and failure process. In PHM community, the uncertainty of estimated RUL is mainly separated into three sources: temporal variability, unit-to-unit variability and measurement variability [10]. These three variabilities are the sources of uncertainty. Temporal variability and unit-to-unit variability involve both epistemic uncertainty and aleatory uncertainty, as their uncertainties can be partially reduced with the increase of degradation data. For measurement variability, its uncertainty cannot be reduced with the increase of degradation information. Therefore, it does not account for epistemic uncertainty. When the degradation data are sufficient, epistemic uncertainty is reduced and these three sources of variability due to aleatory uncertainty can be individually estimated. However, under limited degradation data, epistemic uncertainty is inevitable, and the precise separation of variability of total uncertainty cannot be easily achieved because they jointly influence the degradation data.

For degradation with recovery phenomenon, epistemic uncertainty is inevitable when observations are limited, and it can be summarized from three aspects. First, limited data will cause a lack of knowledge on recognizing all the representative degradation paths and lead to epistemic uncertainty in parameter estimation. Second, the occurrence frequency and amplitude of recovery are two factors associated with epistemic uncertainty. Third, as the model is built based on the historical information of similar components, epistemic uncertainty on similarities between on-site component and historical components cannot be ignored. Therefore, it is important to update the model considering the similarities of different components with the increase of condition monitoring information on on-site component.

To account for epistemic uncertainties mentioned above, first, a new mathematical theory called uncertainty theory [11] has been introduced for degradation modeling and RUL prediction. This theory treats the chance of an event as belief degree and it can be used to quantify epistemic uncertainty. In uncertainty theory, uncertain process can be used to represent degradation trend subject to epistemic uncertainty. Compared with stochastic process, uncertain process could lead to more stable results when dealing with epistemic uncertainty, especially under limited degradation data. Second, the epistemic uncertainty of similarities between on-site component and historical similar components is quantified with proposed parameter update method called similarity based-uncertain weighted least squares estimation method. Third, the impact of epistemic uncertainty caused by recovery phenomenon is reduced with a novel denoising method.

The contributions of this study are summarized as follows:

1) Uncertain process is firstly used for RUL prediction in this paper and a systematic method for RUL prediction based on uncertain process is presented.
2) This paper presents a new uncertain statistical method to update the parameters with real-time monitoring data and epistemic uncertainty of similarities between on-site component and historical similar components is properly quantified.
3) A new denoising method is proposed to deal with recovery phenomenon, possible fluctuations and measurement errors, to which we all refer as noises. Then, the impacts of epistemic uncertainty of recovery phenomenon are reduced.

The remainder of this paper is organized as follows. In Section 2, some applications of uncertainty theory and the recent studies of RUL prediction considering recovery phenomenon are reviewed. In Section 3, the proposed method is presented in detail including degradation modeling, uncertain parameter estimation, uncertain parameter update, denoising method and uncertain simulation for RUL prediction. In Section 4, a case study referring to real lithium-ion battery degradation dataset is conducted to demonstrate the effectiveness of the proposed methodology. Section 5 concludes the paper.

2. Literature review

2.1. Applications of uncertainty theory

For reliability analysis, applying uncertainty theory can compensate for conservatism in the component-level reliability metrics induced by epistemic uncertainty. Besides, it satisfies the duality axiom and avoids the possible paradoxical results encountered in other reliability metrics [12]. Several works have been conducted by employing it to deal with epistemic uncertainty. Zeng et al. [13] developed minimal cut set-based method based on uncertainty theory to calculate belief reliability of coherent systems. Zhang et al. [14] proposed a reliability metric called belief reliability based on uncertainty theory and probability theory. Li et al. [15] introduced uncertainty theory to build up a framework of accelerated degradation testing to evaluate epistemic uncertainty. Hu et al. [16] provided methods of expression and propagation of uncertainty in fault tree analysis based on frequentist probability and uncertainty theory, where frequentist probability was used to express aleatory uncertainty and uncertainty theory was used to represent the epistemic uncertainty.

2.2. Study of recovery phenomenon in PHM community

In the degradation modeling and RUL prediction community, the recovery phenomenon has recently drawn researchers' attention. For lithium-ion batteries, approaches to decouple global degradation and local regeneration from state of health (SOH) time series have been developed. He et al. [17] utilized wavelet analysis to decouple global degradation, local regeneration and fluctuations and used multiscale Gaussian Process Regression (GPR)-based models to fit extracted global degradation trend and to predict local regeneration. Zhou and Huang [18] combined empirical mode decomposition (EMD) and autoregressive integrated moving average model to predict the RUL of lithium-ion batteries. However, these models could not capture random dynamics and characterize the uncertainty in degradation process as stochastic process models did. Some researchers have regarded capacity regeneration as unpredictable disturbance. Olivares et al. [19] took capacity regeneration phenomena (CRP) as an external input to the degradation state space model. Particle filtering and information-theoretic measures were utilized to estimate the RUL of batteries. In [20], locations of CRP were considered as un unobserved latent random variable and CRP were probabilistically and automatically detected. However, these approaches cannot predict the regeneration phenomenon and the prediction errors around these related cycles will increase. Some researchers modified the traditional Wiener process models by taking capacity regeneration phenomenon into consideration. Zhang et al. [21] proposed a prognostic model based on Wiener process and used a two-state semi-Markov model with phase-type distributed interval time to characterize the deteriorating components experiencing a switching operating process between usage and storage process. Xu et al. [22] studied the influence of regeneration phenomenon and proposed a novel RUL prediction method based on Wiener process by using regenerated useful time to model the recovery process. Zhang et al. [23] built a multi-phase stochastic degradation model with random jumps based on Wiener process and developed an approach for model identification based on expectation conditional maximum algorithm. However, stochastic process models mentioned above haven't considered the influence of epistemic uncertainty in degradation modeling and RUL prediction.

For PEMFC, Jouin et al. [24] took into account the recovery phenomenon and developed a new empirical model for charactering power aging. The model was used in a joint particle filter framework and was

applicable with sufficient degradation data. Liu et al. [25] employed wavelet analysis to decompose the original voltage sequence of PEMFCs into sub-waveforms. Then, prognostics was made for the sub-waveforms and combined for the overall prediction. Jouin et al. [26] built empirical models in both learning and prediction phases of the prognostics model by combining three particle filters modules. However, epistemic uncertainty due to limited degradation data hasn't been considered in these methods.

In conclusion, besides the existing literatures on degradation modeling and RUL prediction in consideration of recovery phenomenon, epistemic uncertainty needs further to be dealt with, especially when the degradation data size is limited.

3. Methodology

In this section, the procedures of degradation modeling and RUL prediction are shown. The flowchart of the proposed method is shown in Fig. 1. First, the historical measurements of similar components are used to train the degradation model based on uncertain process. The model parameters are initialized using the uncertain principle of least squares. With the increasing measurements of the on-site component, the proposed similarity based-uncertain weighted least squares estimation method is employed to update the model parameters. In the next stage, a denoising method is proposed to deal with the recovery phenomenon, fluctuations and measurement errors to obtain denoised historical measurements and denoised on-site measurements. These denoised measurements are entered into the degradation model and the parameters of modified models are calculated again. At last, uncertain simulation is developed to calculate the RUL of on-site component.

3.1. Preliminaries

Before the presentation of uncertain process degradation model, some basic definitions and theorems in uncertainty theory are introduced.

Definition 1. [11] An uncertain variable $\mathscr{E}$ is called normal if it has normal uncertain distribution as:

$$\Phi(x) = \left(1 + \exp\left(\frac{\pi(e-x)}{\sqrt{3}\sigma}\right)\right)^{-1}, x \in \mathscr{R} \tag{1}$$

denoted by $\mathscr{N}(e,\sigma)$, where e and σ are real numbers with $\sigma > 0$.

Definition 2. [27] An uncertain process C_t is said to be a Liu process if

(i) $C_0 = 0$ and almost all sample paths are Lipschitz continuous,
(ii) C_t has stationary and independent increments,
(iii) every increment $C_{s+t} - C_t$ is a normal uncertain variable with expected value 0 and variance t^2.

Definition 3. [11] Assume that we have obtained a set of expert's experimental data

$$(x_1, \alpha_1), (x_2, \alpha_2), \ldots, (x_n, \alpha_n)$$

that meet the following consistence condition (perhaps after a rearrangement)

$$\begin{aligned} &x_1 < x_2 < \ldots < x_{n-1} < x_n \\ &0 < \alpha_1 < \alpha_2 < \ldots < \alpha_{n-1} < \alpha_n < 1 \end{aligned}$$

where x_i is the ith experimental data and α_i is the corresponding degree.

Based on those expert's experimental data, Liu suggested an empirical uncertainty distribution:

$$\Phi(x) = \begin{cases} 0 & x < x_1 \\ \alpha_i + \dfrac{(\alpha_{i+1} - \alpha_i)(x - x_i)}{(x_{i+1} - x_i)} & x_i \le x \le x_{i+1} \\ 1 & x > x_n \end{cases} \tag{2}$$

Remark 1. The empirical uncertainty distribution Φ determined by (2) has an expected value:

$$E[\varepsilon] = \frac{\alpha_1 + \alpha_2}{2} x_1 + \sum_{i=2}^{n-1} \frac{\alpha_{i+1} - \alpha_{i-1}}{2} x_i + \left(1 - \frac{\alpha_{n-1} + \alpha_n}{2}\right) x_n \tag{3}$$

If all x_i is nonnegative, then the kth empirical moments are

$$E\left[\varepsilon^k\right] = \alpha_1 x_1^k + \frac{1}{k+1} \sum_{i=1}^{n-1} \sum_{j=0}^{k} (\alpha_{i+1} - \alpha_i) x_i^j x_{i+1}^{k-j} + (1 - \alpha_n) x_n^k \tag{4}$$

Definition 4. [11] Assume that an uncertainty distribution to be determined has a known functional form $\Phi(x|\theta)$ with an unknown parameter θ. In order to estimate the parameter, we can employ the uncertain principle of least squares that minimizes the sum of the squares of the distance of belief degree and the uncertainty distribution. If the data and the belief degrees $(x_1, \alpha_1), (x_2, \alpha_2), \ldots, (x_n, \alpha_n)$ are obtained, then we have:

$$\min_{\theta} \sum_{i=1}^{n} \left(\Phi(x_i|\theta) - \alpha_i\right)^2 \tag{5}$$

The optimal solution $\widehat{\theta}$ is called the least squares estimate of θ.

3.2. Degradation model based on uncertain process

With sufficient observations, the stochastic process models based on probability theory can achieve good results according to the law of large number. If the degradation data size is limited, the influence of epistemic uncertainty in degradation modeling and RUL prediction has to be considered, especially for degradation with recovery phenomenon. Besides, for the commonly used stochastic process, Wiener process,

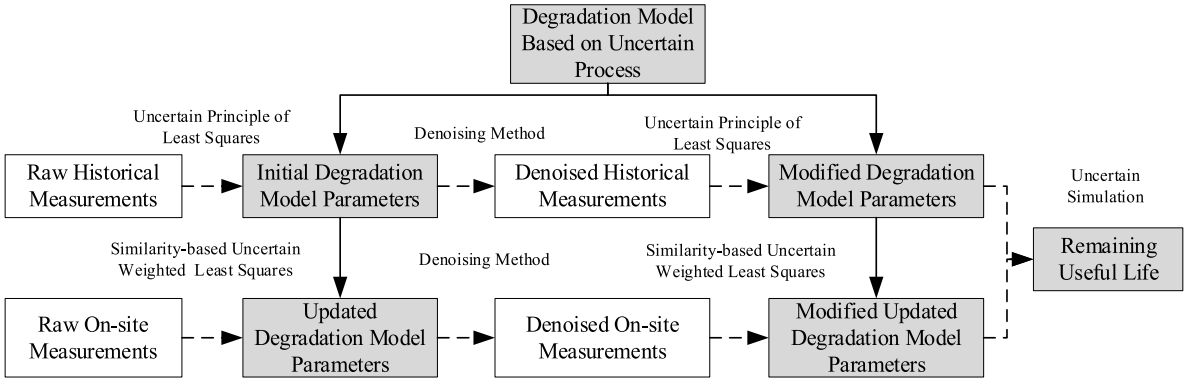

Fig. 1. Flowchart of proposed method.

almost all of its sample paths are non-Lipschitz continuous function, which is not consistent with practice. In this paper, Liu process based on uncertainty theory is employed for degradation modeling, which is a Lipschitz continuous uncertain process with stationary and independent increments.

Let x_i denote the component degradation state at t_i, the degradation model based on uncertain process is described as follows:

$$x_i = x_0 + mt_i^b + \sigma C(t_i^b) \tag{6}$$

where x_0 is the initial component degradation state which is individual-specific, m is the drift parameter, σ is the diffusion parameter, b is the nonlinear parameter, $b > 0$, $C(t_i^b)$ is a Liu process and it can be used to describe Brownian motion in uncertain process, $\sigma C(t_i^b)$ follows an uncertain normal distribution and represents the temporal variability of the uncertain process, mt_i^b describes the severity of the degradation.

According to the proposed degradation model, the degradation increment $x_i - x_{i-1}$ between two time steps t_i and t_{i-1} follows normal uncertainty distribution and can be expressed as:

$$x_i - x_{i-1} \sim \mathcal{N}\left(m\left(t_i^b - t_{i-1}^b\right), \sigma\left(t_i^b - t_{i-1}^b\right)\right) \tag{7}$$

Note that the expected value of degradation state $m(t_i^b - t_{i-1}^b)$ denotes the deterministic degradation trend and the variance of degradation $\sigma(t_i^b - t_{i-1}^b)$ describes the uncertainty caused by the uncertain influential factors.

3.3. Parameter estimation based on uncertain principle of least squares

For the unknown parameters m, σ and b in the uncertain process, uncertain principle of least squares is utilized for their initializations based on available historical measurements. This method minimizes the sum of the squares of the distance between the obtained belief degrees and the assumed uncertainty distribution and involves two steps: belief degree calculation and parameter estimation. Belief degree represents the strength with which you believe an event will happen. It is a subjective concept. In this paper, this subjective measure is calculated based on objective observations, as objective existences are one of the important sources of information for subjective inference [28].

The approximate median rank function is used to calculate the belief degrees in this paper. The procedure for calculating the belief degrees of degradation increments is given in Fig.2.

According to the proposed model, the assumed uncertainty distribution $\Phi_{i,j}$ for increment $z_{j,i}^*$ follows normal uncertainty distribution as (7). After calculation of belief degree α_i^* for Z_i^*, the unknown parameters can be estimated based on uncertain principle of least squares. The objective function Q can be established as follows:

$$\begin{aligned} Q &= \sum_{i=1}^{K}\sum_{j=1}^{N_i}\left(\Phi_{j,i} - \alpha_{j,i}^*\right)^2 \\ &= \sum_{i=1}^{K}\sum_{j=1}^{N_i}\left(\frac{1}{1+\exp\left(\frac{\pi\left[m\left(t_j^b - t_{j-1}^b\right) - z_{j,i}^*\right]}{\sqrt{3}\sigma\left(t_j^b - t_{j-1}^b\right)}\right)} - \alpha_{j,i}^*\right)^2 \end{aligned} \tag{8}$$

Through minimizing the objective function Q, the estimates of m, σ and b can be obtained.

3.4. Parameter update based on similarity

The model based on available historical measurements can reflect the degradation trend of similar components. Note that similar components also have unit-to-unit variation due to the manufacturing process variance. Therefore, it is necessary to consider the differences between

Input: Raw degradation incremental data for each historical component: the increments of i^{th} historical component are denoted as $Z_i^* = \left\{z_{1,i}^*, z_{2,i}^*, \cdots, \boldsymbol{z}_{j,i}^* \cdots \boldsymbol{z}_{N_i,i}^*\right\}$, $j = 1,2,\ldots N_i$, $i = 1,2,\ldots K$, where N_i is the number of degradation data for i^{th} component, K is the number of historical components.

Output: The belief degree series α_i^* for each degradation incremental series Z_i^*, $i = 1,2,\ldots K$.

1. **For** $i = 1,\ldots,K$, proceed as follows:
2. Sort Z_i^* from small to large, and obtain the sorted series $Z_i^\circ = \left\{z_{1,i}^\circ, z_{2,i}^\circ, \cdots, \boldsymbol{z}_{j,i}^\circ \cdots \boldsymbol{z}_{N_i,i}^\circ\right\}, \boldsymbol{j = 1,2,\ldots N_i}$.
3. Calculate the belief degree for each increment $z_{j,i}^\circ$ based on its rank as $\alpha_{j,i}^\circ = \frac{j - 0.3}{N_i + 0.4}$. Then, obtain the belief degree series $\alpha_i^\circ = \left\{\alpha_{1,i}^\circ, \alpha_{2,i}^\circ, \cdots, \boldsymbol{\alpha}_{j,i}^\circ, \cdots \boldsymbol{\alpha}_{N_i,i}^\circ\right\}$, $\boldsymbol{j = 1,2,\ldots N_i}$.
4. Arrange belief degree series α_i° based on the initial degradation incremental series Z_i^* as $\alpha_i^* = \left\{\alpha_{1,i}^*, \alpha_{2,i}^*, \cdots, \boldsymbol{\alpha}_{j,i}^*, \cdots \boldsymbol{\alpha}_{N_i,i}^*\right\}$, $\boldsymbol{j = 1,2,\cdots N_i}$.
5. **End for.**

Fig. 2. Procedure for calculating belief degree.

measurements of on-site component and historical measurements of similar components. As the measurements of on-site component will accumulate gradually, the model parameters can be updated to adapt to the degradation characteristics of on-site component. In this paper, a similarity based-uncertain weighted least squares estimation method is proposed to update the model parameters with real-time monitoring data. The weight in proposed method is proportional to the similarity degree between on-site component and historical components. In this way, the information regarding to the most similar historical components can be filtered, and the updated model for on-site component will become more accurate.

In the proposed method, the objective function shown in (9) is modified by integrating similarity as follows:

$$Q = \sum_{i=1}^{K}\sum_{j=1}^{N_i}\omega_i\left(\Phi_{j,i} - \alpha_{j,i}^*\right)^2 \tag{9}$$

where ω_i is the weight calculated based on the similarity of ith historical components and on-site component. Note that the larger ω_i is, the more similar ith historical component is to on-site component. Assuming there are K historical components, their raw degradation measurements and degradation incremental data are expressed as $Z_i = \{z_{1,i}, z_{2,i}, \cdots z_{N_i,i}\}$ and $Z_i^* = \{z_{1,i}^*, z_{2,i}^*, \cdots z_{N_i,i}^*\}$, $i = 1,2,\ldots K$. The raw degradation measurements and degradation incremental data of on-site component at current operating time t are expressed as $Y = \{y_1, y_2, \cdots y_t\}$ and $Y^* = \{y_1^*, y_2^*, \cdots y_t^*\}$. The calculation of ω_i is as follows. First, a sliding time window with length L is utilized to generate segments from measurements of historical components and on-site component. The obtained segments of the ith historical components and on-site component are expressed as $\mathbf{z}_{L,i}, \mathbf{z}_{L,i}^*, \mathbf{y}_{L,t}$, and $\mathbf{y}_{L,t}^*$, respectively, $\mathbf{z}_{L,i} = \{\mathbf{z}_{1\_L,i}, \ldots \mathbf{z}_{j\_j+L-1,i}\ldots, \mathbf{z}_{N_i-L+1\_N_i,i}\}, \mathbf{z}_{L,i}^* = \{\mathbf{z}_{1\_L,i}^*, \ldots \mathbf{z}_{j\_j+L-1,i}^*\ldots, \mathbf{z}_{N_i-L+1\_N_i,i}^*\}$, where $\mathbf{z}_{j\_j+L-1,i}$ and $\mathbf{z}_{j\_j+L-1,i}^* \boldsymbol{j} = 1, 2, \ldots \boldsymbol{N_i - L + 1}$, are measurements collected from time

point j to time point $j+L-1$ of Z_i and Z_i^* respectively, $\mathbf{y}_{L,t} = \{y_{t-L+1}, y_{t-L+2}\cdots y_{t-1}, y_t\}$, and $\mathbf{y}_{L,t}^* = \{y_{t-L+1}^*, y_{t-L+2}^*\cdots y_t^*\}$.

Second, the Euclidean distance and cosine distance between $\mathbf{z}_{L,i}$,$\mathbf{z}_{L,i}^*$,$\mathbf{y}_{L,t}$, and $\mathbf{y}_{L,t}^*$ are calculated as follows:

$$\begin{aligned} d_{1,j,i} &= \sqrt{\sum_L \left(\mathbf{z}_{j-j+L-1,i}^* - \mathbf{y}_{L,t}^*\right)^2} \\ d_{2,j,i} &= 1 - \frac{\mathbf{z}_{j-j+L-1,i}\cdot \mathbf{y}_{L,t}}{\sqrt{\sum_L \mathbf{z}_{j-j+L-1,i}^2}\sqrt{\sum_L \mathbf{y}_{L,t}^2}} \end{aligned} \quad \begin{matrix} j = 1,2,\ldots N_i - L + 1, \\ i = 1,2,\ldots K \end{matrix} \tag{10}$$

Euclidean distance can reflect the distance similarity between increments and cosine distance can reflect the spatial direction similarity of raw data [29]. Larger index indicates less similarity between the historical component and on-site component. Therefore, the reciprocal values of $d_{1,j,i}$ and $d_{2,j,i}$, are used to represent distance similarity and direction similarity, respectively, as follows:

$$\begin{aligned} E_{1,j,i} &= \frac{1}{d_{1,j,i}} \\ E_{2,j,i} &= \frac{1}{d_{2,j,i}} \end{aligned} , j = 1,2,\ldots N_i - L + 1, i = 1,2,\ldots,K \tag{11}$$

Then, the maximum similarity indexes $S_{1,i}$ and $S_{2,i}$ are chosen as the eventual similarity indexes between ith historical components and on-site component.

$$\begin{aligned} S_{1,i} &= \max_j\left(E_{1,j,i}\right) \\ S_{2,i} &= \max_j\left(E_{2,j,i}\right) \end{aligned} , j = 1,2,\ldots,N_i - L + 1, i = 1,2,\ldots,K \tag{12}$$

In the next step, $S_{1,i}$ and $S_{2,i}$ are normalized to $(0,1)$ as follows:

$$\begin{aligned} S_{1,i}^* &= \frac{S_{1,i}}{\sum_{i=1}^{K} S_{1,i}} \\ S_{2,i}^* &= \frac{S_{2,i}}{\sum_{i=1}^{K} S_{2,i}} \end{aligned} , i = 1,2,\ldots K \tag{13}$$

$$\omega_i = \frac{1}{2}S_{1,i}^* + \frac{1}{2}S_{2,i}^*, i = 1,2,\ldots K \tag{14}$$

Through minimizing the objective function Q as (9), we can update the model parameters m, σ and b.

3.5. Denoising method

In degradation modeling, the measurements of components are assumed to indicate their intrinsic degradation state. However, recovery phenomena, fluctuations and measurement errors will lead noises to the measurements. Therefore, a denoising method is proposed to reduce the effects of noises, where the rule of consistency [30] is assumed and implemented in the denoising process. Consistency indicates that a component degradation state will change slightly during a short period of time.

The procedure of denoising method for measurements of historical components and on-site component is given in Fig.3.

In the proposed denoising method, the original measurements are firstly smoothed to reduce the variation through steps 1–4. The increments follow normal uncertainty distributions as (7) and they are restricted to the range of one-time standard deviation by calculating their expectations, upper and lower bounds as follows:

$$x_{i+1}^{'} = x_i + m\left(t_{i+1}^b - t_i^b\right) \tag{15}$$

Input: Measurements of components $X = \{x_1, x_2, \cdots, x_{N-1}, x_N\}$; model parameter set $\Phi = \{\mathbf{m}, \boldsymbol{\sigma}, \mathbf{b}\}$; length of window M.

Output: Denoised measurements of components $X^* = \{x_1^*, x_2^*, \cdots, x_N^*\}$.

1. **For** $i = 1,2,\ldots N-1$, proceed as follows:
2. Calculate the expectation $x_{i+1}^{'}$, upper bounds $\overline{x}_{i+1}$ and lower bounds $\underline{x}_{i+1}$ for $i+1^{th}$ measurement based on i^{th} measurements x_i according to (15)-(17).
3. **If** $x_{i+1} > \overline{x}_{i+1}$, replace x_{i+1} with $\overline{x}_{i+1}$
   ELSE IF $x_{i+1} < \underline{x}_{i+1}$, replace x_{i+1} with $\underline{x}_{i+1}$
   Then, the modified measurements are obtained.
4. **End For**
5. **For** $i = M+1, M+2,\ldots N-1$, proceed as follows:
6. For linear/nonlinear model, use linear/nonlinear regression to fit the M measurements $\{x_{i-M}, x_{i-M+1}, \cdots x_{i-2}, x_{i-1}\}$.
7. Calculate the forecast value x_i^* by the regression equation and replace original x_i with x_i^* to satisfy consistency.
8. For measurements of historical components, calculate the forecast value x_{i-M-1}^* by the regression equation and replace $x_{i\text{-}M\text{-}1}$ with x_{i-M-1}^*. In this way, the previous measurements can be rectified based on the afterwards degradation monitoring information.
9. **End for.**

Fig. 3. The procedure of the proposed denoising method.

$$\overline{x}_{i+1} = x_i + m\left(t_{i+1}^b - t_i^b\right) + \sigma\left(t_{i+1}^b - t_i^b\right) \tag{16}$$

$$\underline{x}_{i+1} = x_i + m\left(t_{i+1}^b - t_i^b\right) - \sigma\left(t_{i+1}^b - t_i^b\right) \tag{17}$$

For normal uncertainty distribution like (1), the possibility of lying within $e \pm \sigma$can be obtained as follows:

$$Ps\{e - \sigma \le X \le e + \sigma\} \approx 0.7196 \tag{18}$$

Then, linear/nonlinear regression is built to predict the denoised measurement at next time point for linear/nonlinear model. In this way, the consistency is guaranteed. Note that for the historical components, the previously smoothed measurements can be further rectified in step 8 for future model parameter estimation. In contrast, measurements of on-site component do not need the step 8, as adjustment for previous measurements is not helpful to real-time prediction. In Fig. 4, the procedure of proposed denoising method is illustrated. The range of one-time standard deviation depends on the value of the previous measurement and model parameters as (16)-(17). Regression method is used to obtain the final denoised measurements.

Fig. 5 gives an example of applying the proposed denoising method to the capacity measurements of lithium-ion batteries. It can be observed that denoised degradation measures have much lower variations and higher closeness to the true capacity than the raw capacity since the former.

3.6. RUL prediction based on uncertain simulation

After denoising procedure, parameters of degradation model can be updated by using the denoised measurements. Then, uncertain simulation is employed for RUL prediction. We generate M simulated degradation paths at each time point. When the degradation path reaches the pre-determined threshold, the component is considered to have failed.

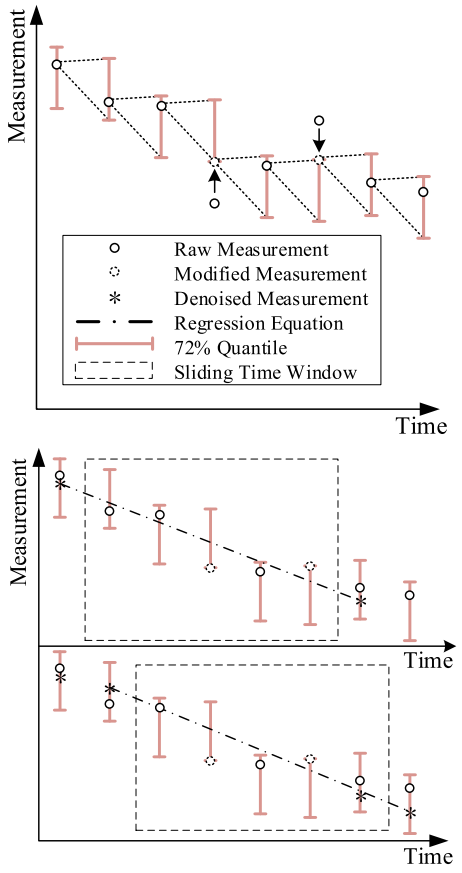

Fig. 4. Illustration of denoising procedure.

The simulated degradation paths are produced using simulation method as follows:

Let *thre* be the failure threshold for the degradation process. Given model parameters at time t, m_t,σ_t and b_t, the procedure of uncertain simulation to calculate RUL is given in Fig. 6.

4. Case study

In this section, a case study of a real lithium-ion battery degradation dataset is used to verify the effectiveness of the proposed method.

4.1. Battery degradation dataset

The lithium-ion battery degradation dataset is provided by the Prognostics CoE at NASA Ames. A set of four Li-ion batteries (5#, 6#, 7# and 18#) were run through three different operational profiles (charge, discharge and impedance) at room temperature (24 °C). All the test cells undergo the same constant current and voltage (CC&CV) charging regime: charging was carried out in a constant current (CC) mode at 1.5A until the battery voltage reached the cell upper voltage limit of 4.2V, and then continued in a constant voltage (CV) mode until the charge current dropped to 20mA. Discharge was carried out at a constant current (CC) level of 2A until the battery voltage fell to 2.7V, 2.5V, 2.2V and 2.5V for batteries 5#, 6#, 7#, and 18# respectively. Impedance measurement was carried out through an electrochemical impedance spectroscopy (EIS) frequency sweep from 0.1Hz to 5kHz. Repeated charge and discharge cycles result in accelerated aging of the batteries while impedance measurements provide insight into the internal battery parameters that change as aging progresses. Based on the previous analysis of available performance measures of the lithium-ion batteries, the capacity can be selected as a comprehensive indicator to characterize the long-term degradation process induced by the charge-discharge operational cycle. The batteries were assumed to have failed when the batteries' capacity reached the failure threshold, which was 70% of the initial capacity.

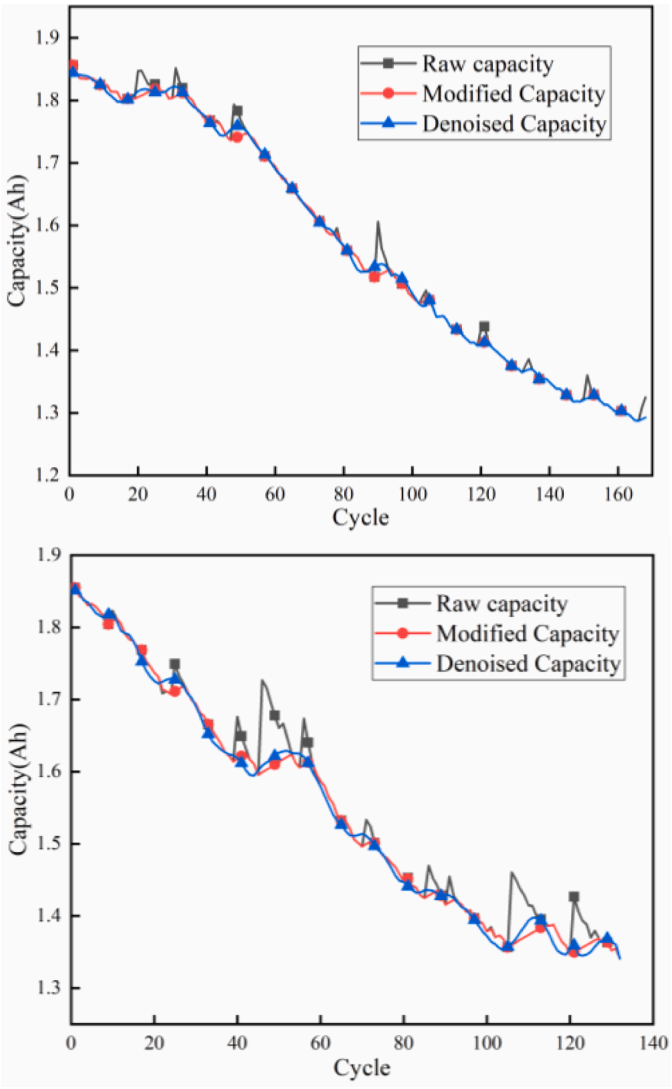

Fig. 5. Denoised battery degradation measurements.

4.2. Uncertain process degradation modeling

For degradation modeling, epistemic uncertainty has to be considered especially when sample size is not large. In this case study, only four batteries are tested and this is a typical small sample problem. To verify the validity of the proposed method, we select two batteries in turn for training and the others for testing. The combinations of batteries for training are presented in Table 1.

The degradation paths of batteries are shown in Fig. 7. In this paper, both linear uncertain process and nonlinear uncertain process are utilized to model the degradation. The distributions followed by the degradation increments in the linear uncertain process and the nonlinear uncertain process are shown in (19) and (20), respectively, as follows:

$$x_i - x_{i-1} \sim \mathcal{N}(m(t_i - t_{i-1}), \sigma(t_i - t_{i-1})) \tag{19}$$

$$x_i - x_{i-1} \sim \mathcal{N}\left(m\left(t_i^b - t_{i-1}^b\right), \sigma\left(t_i^b - t_{i-1}^b\right)\right) \tag{20}$$

Input: Measurement value x_t at time t; threshold $thre$; parameters m_t, σ_t and b_t; interval Δt between two consecutive observation time point; number of iterations of simulation M.

Output: RUL at time t.

1. **For** $i = 1, 2, \ldots, M$, proceed as follows:
2. **Let** $x = x_t$, $n = 1$
3. **While** x is larger than $thre$, do the following:
4. Generate a uniform random number f subject to 0-1 distribution.
5. Generate the increment with parameters m_t, σ_t and b_t

$$\Delta x \sim N\left(m_t\left[(t+n)^{b_t}-(t+n-1)^{b_t}\right], \sigma_t^2\left[(t+n)^{b_t}-(t+n-1)^{b_t}\right]^2\right)$$

with the equation as follows:

$$\Delta x = \left[(t+n)^{b_t}-(t+n-1)^{b_t}\right]\left(m_t + \frac{\sigma_t\sqrt{3}}{\pi}\ln\frac{f}{1-f}\right).$$

6. Let $x = x + \Delta x$; $n = n + 1$
7. **End While**
8. The i^{th} RUL can be calculated as $RUL_i = n * \Delta t$.
9. **End for.**
10. Calculate the average of M RULs according to (3) and get the final RUL at time t

Fig. 6. Uncertain simulation procedure.

Table 1
The combinations of batteries for training.

Combination
1&2 (A1), 1&3 (A2), 1&4 (A3), 2&3 (A4), 2&4 (A5), 3&4 (A6)

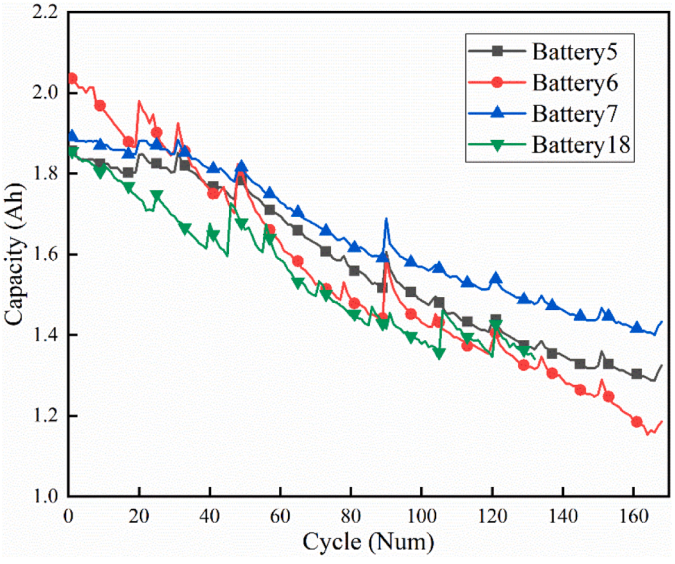

Fig. 7. Degradation of battery capacity degradation.

4.3. Parameter estimation and measurement denoising

First, unknown parameters of the linear and nonlinear uncertain process are initialized as shown in Tables 2 and 3, respectively. For comparison, the results of parameter initialization after denoising procedure are included as well. From Tables 2 and 3, it is obvious that the standard deviations σ of increments after denoising are smaller than those before denoising, which proves that the proposed denoising method has alleviated the effects of noises in raw measurements. After initialization, the model parameters can be updated using monitored data of on-site battery.

Table 2
Parameter initialization in linear uncertain process.

Type	Parameter before denoising		Parameter after denoising	
	m	σ	m	σ
A1	−0.0064	0.0099	−0.0043	0.0067
A2	−0.0044	0.0064	−0.0033	0.0041
A3	−0.0062	0.0084	−0.0037	0.0053
A4	−0.0057	0.0104	−0.0039	0.0062
A5	−0.0092	0.0086	−0.0044	0.0061
A6	−0.0055	0.0088	−0.0034	0.0051

Table 3
Parameter initialization in nonlinear uncertain process.

Type	Parameter before denoising			Parameter after denoising		
	m	σ	b	m	σ	b
A1	−0.0085	0.0128	0.9400	−0.0082	0.0102	0.8668
A2	−0.0043	0.0063	1.0041	−0.0030	0.0022	0.9932
A3	−0.0077	0.0103	0.9555	−0.0040	0.0040	0.9664
A4	−0.0093	0.0163	0.8991	−0.0099	0.0099	0.7866
A5	−0.0090	0.0085	1.0019	−0.0040	0.0040	1.0214
A6	−0.0080	0.0125	0.9263	−0.0044	0.0049	0.9247

From Fig. 7, it is obvious that the degradation increments in regeneration cycles are different than the others. Therefore, it is necessary to apply the denoising procedure to alleviate their effects. Based on the degradation model built using original measurements, the denoised measurements can be obtained according to the procedure shown in Fig. 3. Original and denoised measurements of batteries 5# (linear model) and 18# (nonlinear model) are shown in Fig. 5, where the variations in regeneration cycles are rectified in order to improve the prediction results afterwards.

4.4. RUL prediction and discussion

After parameter update with the measurements of on-site battery, uncertain simulation procedure proposed in Section 3-5 is used to predict RUL. For comparison, the Wiener process is also applied to predict RUL and their prediction results are quantitatively compared. Three commonly used accuracy index in RUL prediction, RMSE, Median SE, and Maximum SE are chosen as the comparison criterion, its expressions are as follows:

$$RMSE = \sqrt{\frac{1}{T}\sum_{j=1}^{T}\left(\frac{1}{\sum_{k=1}^{K_{test}}\left(N_{jk}^{end}-N_{jk}^{start}\right)}\sum_{k=1}^{K_{test}}\sum_{i=N_{jk}^{start}}^{N_{jk}^{end}}\left(t_{ijk}-\bar{t}_{ijk}\right)^2\right)} \tag{21}$$

$$MedianSE = \sqrt{\frac{1}{T}\sum_{j=1}^{T}\left(\frac{1}{K_{test}}\sum_{k=1}^{K_{test}}median_{i=N_{jk}^{start}}^{N_{jk}^{end}}\left(t_{ijk}-\bar{t}_{ijk}\right)^2\right)} \tag{22}$$

$$MaximumSE = \sqrt{\frac{1}{T}\sum_{j=1}^{T}\left(\frac{1}{K_{test}}\sum_{k=1}^{K_{test}}\max_{i=N_{jk}^{start}}^{N_{jk}^{end}}\left(t_{ijk}-\bar{t}_{ijk}\right)^2\right)} \tag{23}$$

where T is the number of combinations (in this case study $T = C_4^2 = 6$), K_{test} is the number of components to be predicted, N_{jk}^{start} and N_{jk}^{end} is the starting and ending time points, respectively, to predict RUL for kth component with the jth combination training set, t_{ijk} represents the related predicted RUL and $\bar{t}_{ijk}$ represents the actual RUL.

The procedure of RUL prediction based on Wiener process are the

same as that based on uncertain process, including degradation modeling, parameter estimation, parameter update, measurement denoising, parameter estimation with denoised measurements and RUL prediction. In contrast to uncertain process, the parameters in stochastic process are estimated through maximum likelihood estimation. Besides, for Wiener process model, $1.1-\sigma$ principle is used in denoising procedure. Because for a normal distribution $N(\mu,\sigma)$ in probability theory, $\Pr\{\mu-1.1\times\sigma\le X\le\mu+1.1\times\sigma\}\approx 0.7287$ which is close to (18).

Besides, to analyze the effects of sliding time window in similarity quantification, that with different lengths are also applied for RUL prediction. The overall RMSE results are given in Table 4, where the RUL prediction accuracies for total life cycle and the last 50 cycles are presented. The results of Median SE and Maximum SE regarding total life cycle are presented in Table 5 as well.

The RMSE results over time are shown in Fig. 8 where the prediction accuracy changes with cycles. Overall, the proposed RUL prediction method based on nonlinear uncertain process have achieved better results and uncertain process generally outperforms stochastic process for this case study, especially when the battery is close to failure. Note that the RUL prediction accuracy is more important when a component is close to failure, because operators could allocate the maintenance resources accordingly. The results of median SE and maximum SE in Table 5 show that the uncertain process outperforms stochastic process as well.

Furthermore, to validate the effectiveness of the proposed denoising method, the RUL prediction results over total life cycle with/without denoising procedure are compared in Table 6. It can be observed that the proposed denoising method can alleviate the effects of noises due to recovery phenomenon, fluctuations and measurement errors, and improve the prediction accuracy. The RMSE results over time without denoising procedure are shown in Fig. 9, it can be observed that the prediction accuracy of stochastic process has experienced abrupt changes induced by capacity recovery phenomenon, whereas that of uncertain process doesn't, and the prediction accuracy of uncertain process has improved with accumulated measurements on the on-site component, which indicates that the epistemic uncertainty has been gradually reduced with the accumulation of knowledge. This is because that uncertain process is more robust to noisy measurements in consideration of epistemic uncertainty and can achieve more stable results, which is an ideal feature for RUL prediction especially when degradation data size is limited.

Besides, the upper and lower bound of confidence intervals with 90% confidence level are presented in Fig. 10. We can see from the figure that the confidence intervals of nonlinear uncertain process are narrower than those of nonlinear stochastic process at the same confidence level, which proves the stability of the uncertain process when the epistemic uncertainty plays an important role in degradation modeling.

5. Conclusions

In this paper, a systematic method for degradation modeling and RUL prediction based on uncertain process is proposed for degradation with recovery phenomenon. The uncertain process is adopted to predict the RUL for the first time. A novel parameter estimation method is proposed to update the model parameters. Besides, a denoising method is developed to ease the impacts of recovery phenomenon, possible fluctuations and measurement errors. The results of the practical case study referring to battery degradation show that the proposed RUL prediction method achieves less prediction errors than the traditional Wiener process model.

As future research, the systematic and adaptive procedure to determine the hyper-parameters in the algorithm needs to be further explored, including the length of sliding window, weights of two distance indexes, etc. Secondly, other parameter update methods and denoising methods can be investigated to further improve the RUL prediction accuracy. Thirdly, when the degradation has recovery phenomenon and the degradation trend of component is affected by the

Table 4
RMSE results of RUL prediction.

Degradation model	Time horizon	Window length		
		10	20	30
Linear stochastic process	Total Life cycle	20.09	**18.16**	16.78
Linear uncertain process		17.44	18.33	18.10
Nonlinear stochastic process		21.61	27.77	23.18
Nonlinear uncertain process		**17.21**	18.84	**16.64**
Linear stochastic process	Last 50 cycles	12.02	12.30	12.60
Linear uncertain process		10.96	11.55	12.26
Nonlinear stochastic process		14.06	18.11	16.29
Nonlinear uncertain process		**9.95**	**10.15**	**11.92**

Table 5
Median SE and Maximum SE results of RUL prediction.

Degradation model	Criterion	Window length		
		10	20	30
Linear stochastic process	Median SE	10.81	11.33	10.94
Linear uncertain process		8.83	11.04	11.43
Nonlinear stochastic process		8.65	15.51	11.66
Nonlinear uncertain process		**8.53**	**7.61**	**10.29**
Linear stochastic process	Maximum SE	55.19	55.13	55.88
Linear uncertain process		**47.35**	**50.83**	54.72
Nonlinear stochastic process		64.72	62.29	63.90
Nonlinear uncertain process		49.13	51.34	**50.87**

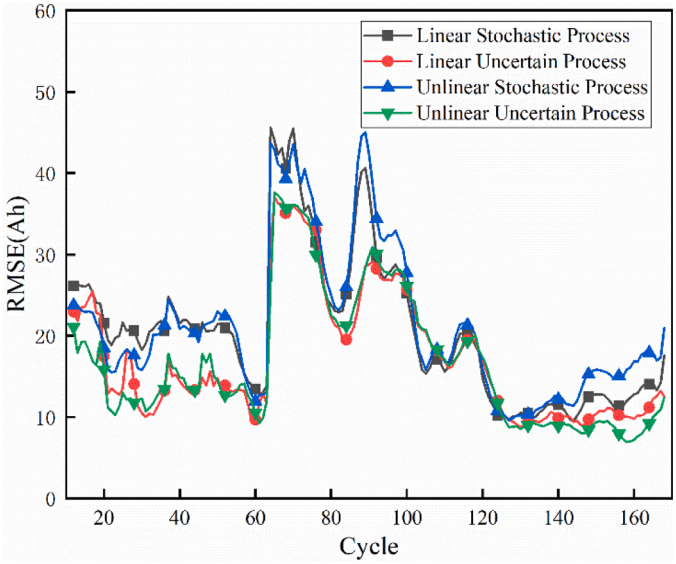

Fig. 8. RMSE results over time.

Table 6
RMSE results of RUL prediction over total life cycle with/without measurement denoising.

Degradation model	Denoising procedure	Window length		
		10	20	30
Linear stochastic process	Yes	20.09	18.16	16.78
Linear uncertain process		17.44	18.33	18.10
Nonlinear stochastic process		21.61	27.77	23.18
Nonlinear uncertain process		17.21	18.84	16.64
Linear stochastic process	No	24.82	24.87	24.95
Linear uncertain process		33.24	32.90	33.17
Nonlinear stochastic process		35.97	35.98	35.95
Nonlinear uncertain process		27.17	27.14	27.18

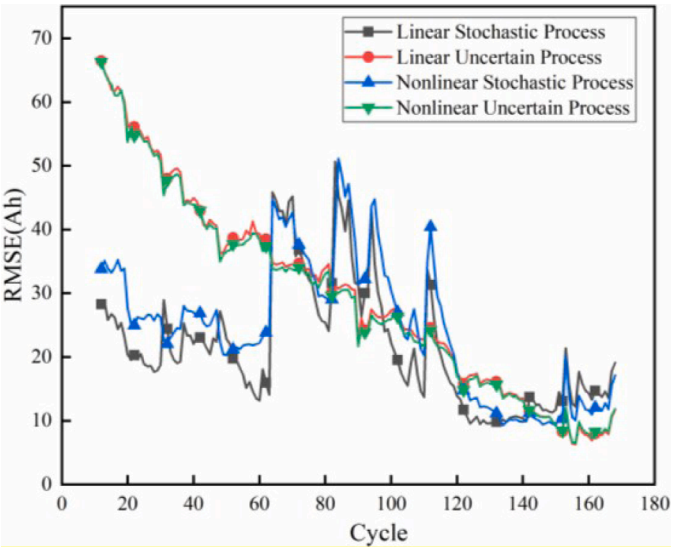

Fig. 9. RMSE results over time without denoising procedure.

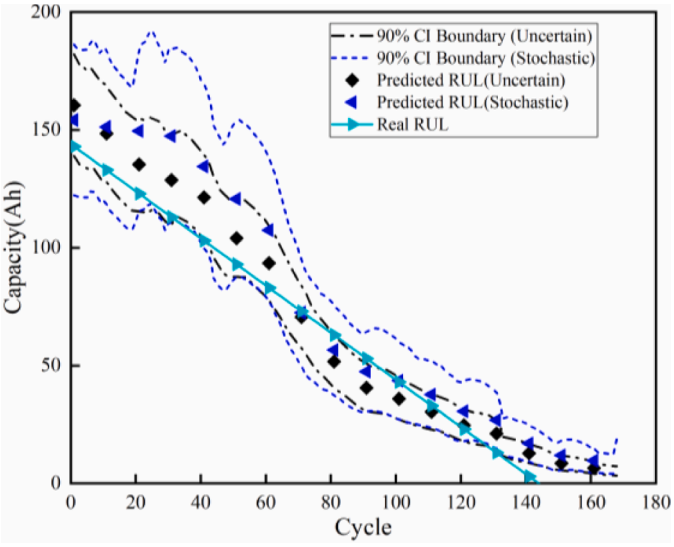

Fig. 10. Confidence intervals of uncertain process and stochastic process.

recovery phenomenon, how to find suitable model to quantify the process is a future direction. Lastly, recovery phenomenon can be used in the future to improve the prediction accuracy.

Declaration of Competing Interest

We declare that we do not have any commercial or associative interest that represents a conflict of interest in connection with the work submitted.

Acknowledgements

This study was supported by the National Natural Science Foundation of China under Grant 51875016, and National Natural Science Foundation of China under Grant 62073009.

References

[1] Bae SJ, Mun BM, Chang W, Vidakovic B. Condition monitoring of a steam turbine generator using wavelet spectrum based control chart. Reliab Eng Syst Saf 2019; 184:13–20.
[2] Lei Y, Li N, Guo L, Li N, Yan T, Lin J. Machinery health prognostics: a systematic review from data acquisition to RUL prediction. Mech Syst Signal Proc 2018;104: 799–834.
[3] Lin YH, Li YF, Zio E. Integrating random shocks into multistate physics models of degradation processes for component reliability assessment. IEEE Trans Reliab 2015;64:154–66.
[4] Chiachio J, Jalon ML, Chiachio M, Kolios A. A Markov chains prognostics framework for complex degradation processes. Reliab Eng Syst Saf 2020;195:10.
[5] Meng HX, Li YF. A review on prognostics and health management (PHM) methods of lithium-ion batteries. Renew Sustain Energy Rev 2019:116.
[6] Hao SH, Jun Y, Berenguer C. Degradation analysis based on an extended inverse Gaussian process model with skew-normal random effects and measurement errors. Reliab Eng Syst Saf 2019;189:261–70.
[7] Kleeberger VB, Barke M, Werner C, Schmitt-Landsiedel D, Schlichtmann U. A compact model for NBTI degradation and recovery under use-profile variations and its application to aging analysis of digital integrated circuits. Microelectron Reliab 2014;54:1083–9.
[8] Barré A, Suard F, Gérard M, Montaru M, Riu D. Statistical analysis for understanding and predicting battery degradations in real-life electric vehicle use. J Power Sources 2014;245:846–56.
[9] Jouin M, Gouriveau R, Hissel D, Péra M-C, Zerhouni N. Degradations analysis and aging modeling for health assessment and prognostics of PEMFC. Reliab Eng Syst Saf 2016;148:78–95.
[10] Si XS, Wang WB, Hu CH, Zhou DH. Estimating remaining useful life with three-source variability in degradation modeling. IEEE Trans Reliab 2014;63:167–90.
[11] Baoding L. Uncertainty theory. 5th ed. Berlin Heidelberg: Springer; 2018.
[12] Kang R, Zhang Q, Zeng Z, Zio E, Li X. Measuring reliability under epistemic uncertainty: review on non-probabilistic reliability metrics. Chin J Aeronaut 2016; 29:571–9.
[13] Zeng Z, Kang R, Wen M, Zio E. Uncertainty theory as a basis for belief reliability. Inf Sci 2018;429:26–36.
[14] Zhang Q, Kang R, Wen M. Belief reliability for uncertain random systems. IEEE Trans Fuzzy Syst 2018;26:3605–14.
[15] Li XY, Wu JP, Liu L, Wen ML, Kang R. Modeling accelerated degradation data based on the uncertain process. IEEE Trans Fuzzy Syst 2019;27:1532–42.
[16] Hu LH, Kang R, Pan X, Zuo DJ. Risk assessment of uncertain random system-level-1 and level-2 joint propagation of uncertainty and probability in fault tree analysis. Reliab Eng Syst Saf 2020;198:10.
[17] He YJ, Shen JN, Shen JF, Ma ZF. State of health estimation of lithium-ion batteries: a multiscale Gaussian process regression modeling approach. AIChE J 2015;61: 1589–600.
[18] Zhou Y, Huang M. Lithium-ion batteries remaining useful life prediction based on a mixture of empirical mode decomposition and ARIMA model. Microelectron Reliab 2016;65:265–73.
[19] Orchard ME, Lacalle MS, Olivares BE, Silva JF, Palma-Behnke R, Estévez PA, et al. Information-theoretic measures and sequential Monte Carlo methods for detection of regeneration phenomena in the degradation of lithium-ion battery cells. IEEE Trans Reliab 2015;64:701–9.
[20] Wang D, Kong J-Z, Zhao Y, Tsui K-L. Piecewise model based intelligent prognostics for state of health prediction of rechargeable batteries with capacity regeneration phenomena. Measurement 2019;147:106836.
[21] Zhang Z-X, Si X-S, Hu C-H, Pecht MG. A prognostic model for stochastic degrading systems with state recovery: application to li-ion batteries. IEEE Trans Reliab 2017; 66:1293–308.
[22] Xu X, Yu C, Tang S, Sun X, Si X, Wu L. Remaining useful life prediction of lithium-ion batteries based on wiener processes with considering the relaxation effect. Energies 2019;12:1685.
[23] Zhang J, He X, Si X, Hu C, Zhou D. A novel multi-phase stochastic model for lithium-ion batteries' degradation with regeneration phenomena. Energies 2017; 10:1687.
[24] Jouin M, Gouriveau R, Hissel D, Péra M-C, Zerhouni N. Joint particle filters prognostics for proton exchange membrane fuel cell power prediction at constant current solicitation. IEEE Trans Reliab 2015;65:336–49.
[25] Liu H, Chen J, Hou M, Shao Z, Su H. Data-based short-term prognostics for proton exchange membrane fuel cells. Int J Hydrogen Energy 2017;42:20791–1808.
[26] Jouin M, Gouriveau R, Hissel D, Péra M-C, Zerhouni N. Prognostics of proton exchange membrane fuel cell stack in a particle filtering framework including characterization disturbances and voltage recovery. In: 2014 International conference on prognostics and health management. IEEE; 2014. p. 1–6.
[27] Liu B. Some research problems in uncertainty theory. J Uncertain Syst 2009;3: 3–10.
[28] Press SJ. Subjective and objective Bayesian statistics: principles, models, and applications. John Wiley & Sons; 2009.
[29] Liu Y, Hu X, Zhang W. Remaining useful life prediction based on health index similarity. Reliab Eng Syst Saf 2019;185:502–10.
[30] Yang F, Habibullah MS, Zhang T, Xu Z, Lim P, Nadarajan S. Health index-based prognostics for remaining useful life predictions in electrical machines. IEEE Trans Ind Electron 2016;63:2633–44.